

EFFECT OF L-HISTIDINE ON PHOTOSYNTHESIS OF MAIZE UNDER SALT STRESS

Ji, H. F. – Qi, Y. X. – Zhang, X.* – Yang, G. P.

Ningxia Key Laboratory for the Development and Application of Microbial Resources in Extreme Environments, College of Biological Science and Engineering, North Minzu University, Yinchuan 750021, China

**Corresponding author
e-mail: zhangxiu101@nmu.edu.cn*

(Received 20th Jan 2024; accepted 3rd May 2024)

Abstract. Soil salinization has damaged the soil biological environment and chemical structure, resulting in a decline in soil quality and crop yields, which has caused harm to the ecological environment and human health, and severely hindered the development of the economy. In this experiment, using the 'Ningdan 33' maize seeds as materials, the maize was treated with histidine and salt stress (100 mM NaCl), and photosynthesis, photosynthetic enzyme activity, relative expression of photosynthetic genes of maize were measured. The anatomical structure of the leaves was also observed. The study explored the impact of exogenous histidine treatment on the photosynthesis of maize under salt stress. When the concentration of histidine sprayed on the leaves was 0.5 mM, it had the best effect on promoting photosynthesis in maize under salt stress. 0.5 mM histidine significantly improved the photosynthetic performance (P_N , g_s , E , $Chl\ a/Chl\ b$) of maize under salt stress, significantly improved photosynthesis efficiency (F_v/F_m , $\Delta F/F_m$, q_p were significantly increased. NPQ was significantly decreased), significantly increased the activity of photosynthetic enzymes (PEPC, NADP-ME, PPDK, Rubisco) and the relative expression of photosynthetic genes (*ZmPEPC*, *ZmNADP-ME*, *ZmPPDK*, *ZmRCA*), increased the length of the vascular bundle in the cross-section of the leaf, played a certain protective role on the vascular bundle, and improved the efficiency of material transportation under salt stress. Based on the above analysis, 0.5 mM histidine can significantly improve the tolerance of maize under salt stress, which has great application value for planting maize in saline environments.

Keywords: amino acid, salinization, *Zea mays*, photosynthetic performance, photosynthetic enzymes and genes, leaf anatomy structure

Introduction

Soil salinization is one of the important factors that plague agricultural development worldwide. In abroad sense, we generally refer to soils containing NaCl and Na₂SO₄ as "saline soils". According to the definition of the National Salt Hazards Laboratory of US, saline soil refers to soils with a saturated extract conductivity (EC) higher than 4 dS m⁻¹ and an exchangeable sodium (ESP) content lower than 15%. Through monitoring the global land salinity changes, it is found that Asia is one of the continents most affected by salt, especially the northwest region of China (Hassani et al., 2020). The Food and Agriculture Organization of the United Nations estimates that salt has affected more than 6% of the land area (Ilangumaran and Smith, 2017), and about 20% of the irrigated land worldwide is affected by salt, resulting in direct economic losses of \$12 billion annually, which is a major threat to food security (Tang et al., 2015).

Photosynthesis in plants plays a crucial role in the production of adenosine triphosphate (ATP), which provides the energy needed to fix CO₂ into sugars. Research has shown that under salt stress, the photosynthetic rate, osmotic potential, water potential, transpiration rate, leaf temperature, and relative leaf water content of plants are significantly affected (Sudhir and Murth, 2004). Salt stress can also affect the

components of photosynthetic structures, such as enzymes, photosynthetic pigments, thylakoid membrane proteins, and membrane lipids (Fernández-García et al., 2014). The adverse effects of salt stress on photosynthesis are due to two mechanisms. First, under salt stress, plant stomata close, reducing the intercellular CO₂ concentration. Second, salt stress also causes damage to the photosynthetic membrane system, reducing CO₂ assimilation capacity and damaging photosynthetic pigments (Shu et al., 2012a). All of these abnormalities can lead to a disorder in ATP synthesis, which in turn leads to a deficiency of certain ions due to ion degradation and synthesis inhibition (Othman et al., 2006). Generally, salt stress increases the content of Na⁺ and Cl⁻ in leaves, reduces the content of K⁺, and leads to stomatal closure. The decrease in stomatal opening severely impedes the diffusion of CO₂ from the environment to the chloroplast, resulting in a decrease in intercellular CO₂ concentration and a reduction in photosynthetic rate (Çavuşoğlu et al., 2018). In salt-sensitive plants, salt stress often leads to a decrease in chlorophyll, which is the most important pigment associated with photosynthesis. For example, in pepper (Zhang et al., 2019), soybean (Du et al., 2018), and rice (Turan and Tripathy, 2014), the chlorophyll content decreases after salt stress. In addition, salt stress impairs the function of oxygen-evolving complexes (Ji et al., 2018), hinders the transfer of electrons from plastid quinone A (QA) to plastid quinone B (QB), and damages the function of pigment-protein complexes on thylakoid membranes (Ioannidis et al., 2006), resulting in a decrease in electron transfer efficiency. As a rate-limiting enzyme in photosynthesis, Rubisco is also affected by salt stress. Salt stress reduces the activity of Rubisco, limits the regeneration of RuBP, and thereby reduces the absorption and utilization of CO₂ by plants (Shu et al., 2014). In short, salt stress hinders the photosynthesis of salt-tolerant plants through stomatal limitation and non-stomatal limitation.

The role and anabolic process of histidine in plants were studied relatively late. Research has found that histidine can regulate the biological processes of other unrelated amino acids, and the histidine biosynthesis pathway is linked to many other metabolic pathways, including the metabolism of purine, pyrimidine, pyridine nucleotide, folate, and tryptophan (Noutoshi et al., 2005; Stepansky and Leustek, 2006). In addition, histidine has a role in metal ion chelation and transport. Free histidine can influence nickel concentration in plants, and supplying histidine to plants greatly increases their nickel tolerance and nickel transport ability to buds (Kramer et al., 1996); in some plants, the selective synthesis of histidine gradually increases with increasing copper concentration (Irtelli et al., 2008). Previous studies have found that histidine can improve the salt tolerance of maize roots (Ji et al., 2022), but it is unknown whether histidine has a positive effect on maize photosynthesis under salt stress. This experiment studied the effect of histidine on maize photosynthesis under salt stress, providing relevant theoretical evidence for the application of histidine in saline soil and the cultivation of maize in saline soil.

Materials and methods

Histidine spray treatment

All plant materials used in the experiment were maize variety "Ningdan 33". The seeds of this variety were disinfected with 0.1% HgCl₂, and after disinfection, they were placed in sterile water and stored at 4°C for 12 hours. Subsequently, the seeds were inoculated on a 0.8% agar medium (containing Hoagland nutrient solution) and placed

in a dark incubator with a relative humidity of 35% and a temperature of 28°C. When the young roots grew to 3 cm, the germination was completed. After inoculating the seeds on sterile vermiculite, all of them were watered with Hoagland nutrient solution and cultured in a lighting incubator (relative humidity 35%, 10,000 Lx, 25°C, 4 h; 5000 Lx, 20°C, 3 h; 0 Lx, 18°C, 8 h; 5000 Lx, 20°C, 2 h; 9000 Lx, 25°C, 3 h; 13,000 Lx, 28°C, 4 h). When the seedlings reached the 2-leaf stage, those that grew evenly were selected and transplanted into a nutrient medium for outdoor cultivation. 100 mM NaCl was used as a salt stress treatment group (Ji et al., 2022). Five concentration ranges of 0.005 mM, 0.05 mM, 0.5 mM, 5 mM, and 50 mM were set, and using the principal component analysis (PCA) in IBM SPSS Statistics (v 25), the optimal spray concentration of histidine under salt stress was selected. The spraying time was 10 am, and each time was 50 mL. When the maize grew for 10 days, its relevant indicators were measured. Subsequent experiments were divided into four groups: (1) spraying sterile water (CK0); (2) spraying 0.5 mM histidine (T0); (3) spraying sterile water with salt stress treatment (CK1); (4) spraying 0.5 mM histidine with salt stress treatment (T1).

Photosynthetic performance

The photosynthetic performance of the fourth fully developed functional leaf of maize was measured using the Li-6400 portable photosynthetic device between 9:00-11:00 am. The leaf chamber temperature was set at 26°C, the light intensity was set at 800 $\mu\text{mol}\cdot\text{m}^{-2}\cdot\text{s}^{-1}$, and the CO_2 concentration was set at 400 $\mu\text{mol}\cdot\text{mol}^{-1}$. Net photosynthetic rate (P_N), stomatal conductance (g_s), transpiration rate (E), and intercellular CO_2 concentration (C_i) were directly read by a photosynthesis instrument. Each treatment was setup with six biological replicates. Significant differences between treatments were analyzed using the Duncan method in IBM SPSS Statistics (v 25).

Chlorophyll content

The determination of chlorophyll a (Chl *a*) and chlorophyll b (Chl *b*) content was based on Lichtenthaler and Wellburn (1983). A 0.1 g piece of fully developed functional leaf tissue was taken and immersed in 10 mL of methanol at room temperature in a dark place. During this process, it was shaken thoroughly until the leaf turned completely white. The absorbance values at 653 nm and 666 nm were measured, and the calculation formula is as follows:

$$\text{Chl } a = 15.65 \times A_{666} - 7.34 \times A_{653} \quad (\text{Eq.1})$$

$$\text{Chl } b = 27.05 \times A_{653} - 11.21 \times A_{666} \quad (\text{Eq.2})$$

As maize is a sun growing plant, we use Chl *a*/Chl *b* to represent the relative chlorophyll content. Each treatment was setup with six biological replicates. Significant differences between treatments were analyzed using the Duncan method in IBM SPSS Statistics (v 25).

Chlorophyll fluorescence parameters

The fourth fully developed functional leaf was dark-adapted for 30 minutes, and the chlorophyll fluorescence parameters were measured using the Li-6400 matched

fluorescence leaf chamber. The weak modulated measurement light was set up to measure the minimum initial fluorescence (F_o), a saturated bright light pulse, and to measure the dark-adapted maximum fluorescence (F_m). The leaves were exposed to natural light for 1 h, and then $600 \mu\text{mol}\cdot\text{m}^{-2}\cdot\text{s}^{-1}$ activating light was added. The steady-state fluorescence (F_s) was measured. In the presence of activating light, a saturated strong light pulse was added, and the maximum fluorescence under light (F'_m) was measured. At the moment the activation light turned off, a few seconds of far-infrared light was added to measure the minimum fluorescence (F'_o) under the light. The following parameters were read directly by the photosynthetic instrument. Each treatment was set up with six biological replicates. Significant differences between treatments were analyzed using the Duncan method in IBM SPSS Statistics (v 25).

Maximum photochemical quantum efficiency of PSII:

$$\frac{F_v}{F_m} = \frac{F_m - F_o}{F_m} \quad (\text{Eq.3})$$

PSIIactual photochemical quantum efficiency:

$$\frac{\Delta F}{F'_m} = \frac{F'_m - F_s}{F'_m} \quad (\text{Eq.4})$$

Photochemical quenching coefficient:

$$q_p = \frac{F'_m - F_s}{F'_m - F'_o} \quad (\text{Eq.5})$$

Non-photochemical quenching coefficient:

$$\text{NPQ} = \frac{F_m - F'_m}{F'_m} \quad (\text{Eq.6})$$

Photosynthetic enzyme activity determination

The phosphoenolpyruvate carboxylase (PEPC) activity, NADP-malic enzyme (NADP-ME) activity, phosphoenolpyruvate diphosphokinase (PPDK) activity of maize were all measured using reagent kits from Suzhou Ke Ming Biotechnology Co., Ltd. (Suzhou, China). Ribulose-1,5-bisphosphate carboxylase (Rubisco) activity was determined using an ELISA kit (Kemeng, Suzhou, China). Each treatment was set up with three biological replicates. Significant differences between treatments were analyzed using the Duncan method in IBM SPSS Statistics (v 25).

Gene relative expression detection

Total RNA was extracted from maize tissues using the MiniBEST Universal RNA Extraction Kit (Takara, Beijing, China). 0.1 μg of total RNA was reverse transcribed into cDNA using PrimeScript™ RT reagent kit and gDNA Eraser (Takara, Beijing, China). The RT-qPCR reaction was performed using TB Green Premix Ex Taq™ II kit

(Takara, Beijing, China). The reaction system was: 12.5 µL Premix Ex TaqII, 1 µL of forward primer, 1 µL of reverse primer, 1 µL of cDNA and 9.5 µL of dd H₂O₂. The qPCR thermal cycling was as follows: 95°C for 30 s followed by 40 cycles of 95°C for 5 s, 55°C for 30 s and 72°C for 30 s. Each treatment was set up with three biological replicates. Significant differences between treatments were analyzed using the Duncan method in IBM SPSS Statistics (v 25). The expression level of relative genes was calculated using the $2^{-\Delta\Delta C_t}$ method. *ZmGAPDH* (LOC542367) was used as an internal reference gene. The primer sequences of related genes are shown in *Table S1*.

Anatomical observation of leaf blade

After 10 days of spray treatment, fresh tissues from each treatment were fixed with a fixative for more than 24 hours. The tissues were removed from the fixative and trimmed with a scalpel in a fume hood. The trimmed tissues and corresponding labels were placed in a dehydration box. The dehydration box was placed in a dehydrator and sequentially dehydrated with gradient alcohol: 75% alcohol for 4 hours, 85% alcohol for 2 hours, 90% alcohol for 2 hours, 95% alcohol for 1 hour, anhydrous ethanol I for 30 minutes, anhydrous ethanol II for 30 minutes, ethanol benzene for 10 minutes, xylene I for 10 minutes, xylene II for 10 minutes, 65°C melted paraffin I for 1 hour, 65°C melted paraffin II for 1 hour, and 65°C melted paraffin III for 1 hour. The wax-soaked tissues were embedded in an embedding machine. First, the melted wax was placed in an embedding frame. Before the wax solidified, the tissues were removed from the dehydration box and placed in the embedding frame according to the requirements of the embedding surface and labeled accordingly. It was cooled on a -20°C freezing table. After the wax solidified, the wax block was removed from the embedding frame and trimmed. The trimmed wax block was cooled on a -20°C freezing table and then placed on a paraffin microtome for sectioning at a thickness of approximately 4 µm. The sections were floated on warm water at 40°C in a spreading machine to flatten the tissues. The slides were scooped up with tissue and baked in a 60°C oven. After drying and melting the wax, they were removed and stored at room temperature for future use.

Place the slides in an environmentally friendly dewaxing transparent solution I for 20 minutes, an environmentally friendly dewaxing transparent solution II for 20 minutes, absolute ethanol I for 5 minutes, absolute ethanol II for 5 minutes, and 75% alcohol for 5 minutes, followed by tap water rinsing. After rinsing, place the slides in a plant safranin staining solution for 2 hours, rinse with tap water for 10 seconds, and wash away excess dye. Place the slides in 50%, 70%, and 80% gradient alcohol for 5 seconds each. It is best to place the slides in clean xylene for 5 minutes, followed by neutral gum mounting. Open the slide scanner and panoramic scanner scanning software, place the prepared stained slides on the scanner slide carrier. After scanning, use the CaseViewer 2.4 browsing software to observe.

Data analysis

Image output and statistical analysis were performed using GraphPad Prism (v 9.0) and IBM SPSS Statistics (v 25).

Results

Screening for optimal spray concentration

In order to compare the optimal spraying concentrations, we performed principal component analysis (PCA) of the six metrics for the seven treatments by SPSS, and the KMO and Bartlett's spherical gradient tests (approximate chi-square ≥ 0.6 ; significance ≤ 0.05) indicated that the results of the PCA were relatively reliable. According to the principle that the eigenvalue of principal components is greater than 1, three principal components were extracted in this experiment (*Table 1*). The first principal component eigenvalue was 1.836 with a contribution rate of 30.6%, and the corresponding eigenvectors were Chl *a*/Chl *b* and P_N . The second principal component eigenvalue was 1.463 with a contribution rate of 24.38%, and the corresponding eigenvectors were *E* and C_i . The third principal component eigenvalue is 1.058 with a contribution rate of 17.64 %, and the corresponding eigenvectors were dry weight and P_N . The cumulative contribution rate of the three principal components is 72.624%. The formulae for the three principal components were obtained by dividing each principal component factor by the eigenvalues of the open root sign as coefficients of the equation:

$$y_1 = 0.601 \times x_1 + 0.557 \times x_2 + 0.386 \times x_3 + 0.125 \times x_4 - 0.057 \times x_5 + 0.4 \times x_6 \quad (\text{Eq.7})$$

$$y_2 = -0.147 \times x_1 + 0.088 \times x_2 + 0.183 \times x_3 + 0.692 \times x_4 + 0.646 \times x_5 - 0.201 \times x_6 \quad (\text{Eq.8})$$

$$y_3 = 0.177 \times x_1 - 0.518 \times x_2 - 0.06 \times x_3 - 0.17 \times x_4 + 0.508 \times x_5 + 0.639 \times x_6 \quad (\text{Eq.9})$$

Table 1. Matrix of factor loadings

Index	Principal component I	Principal component II	Principal component III
Chl <i>a</i> /Chl <i>b</i> (1)	0.815	-0.147	0.182
P_N (2)	0.755	0.106	0.533
g_s (3)	0.523	0.221	0.062
<i>E</i> (4)	0.169	0.837	0.175
C_i (5)	-0.077	0.646	0.508
Dry weight (6)	0.542	-0.201	0.639

Substituting the standardized raw data into the above equation, y_1 , y_2 and y_3 were calculated. Combining the contributions of PC₁, PC₂, and PC₃ with y_1 , y_2 and y_3 gives:

$$y = 0.31 \times y_1 + 0.244 \times y_2 + 0.176 \times y_3 \quad (\text{Eq.10})$$

The mean of each treatment score was calculated and based on *Table 2* and *Fig. 1*, we finally concluded that CK0 > 0.5 mM > 5 mM > 0.005 mM > 50 mM > CK1 > 0.05 mM. Under salt stress, the best photosynthetic performance of maize was achieved when histidine was sprayed at a concentration of 0.5 mM.

Table 2. Comprehensive score of each treatment

Treatment	1	2	3	4	5	6	Average	Rank
CK0	0.43	1.17	0.44	0.24	0.38	1.2	0.643	1
50 mM	-0.42	0.37	-0.53	0.51	-0.4	-0.58	-0.175	5
5 mM	0.19	0.31	-0.11	0.6	0.44	-0.27	0.193	3
0.5 mM	-0.34	-0.58	0.41	0.61	0.74	0.74	0.263	2
0.05 mM	-0.51	-0.59	0	-0.45	-0.58	-0.77	-0.483	7
0.005 mM	-0.44	-0.48	-0.17	0.32	0.68	0.09	0	4
CK1	-0.72	-0.69	-0.12	0.07	-0.79	-0.39	-0.44	6

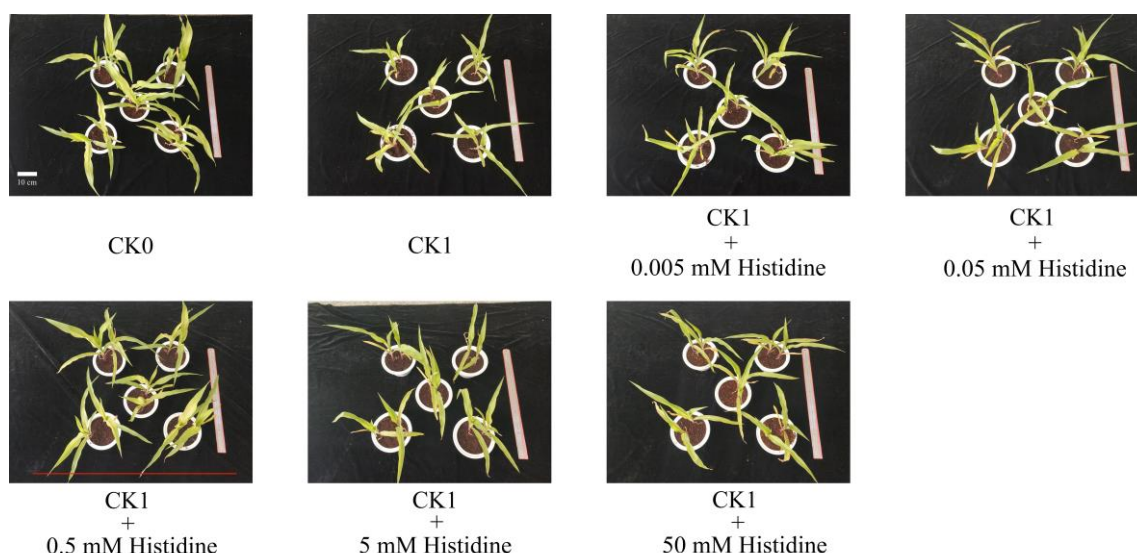


Figure 1. Apparent differences of potted maize sprayed with different concentrations of histidine. The treatment indicated by the red line is the best concentration for spraying histidine

Effect of histidine on the photosynthetic performance of maize

To assess the effect of salinity on plant photosynthesis, we investigated parameters related to photosynthesis. *Fig. 2* shows that salt stress treatments significantly affected photosynthesis in maize, with significant reductions in P_N , g_s , C_i and E . Under normal conditions, spraying 0.5 mM histidine had no significant effect on the photosynthetic performance of maize. Under salt stress, all indices were improved after spraying 0.5 mM histidine. Among them, P_N , g_s and E showed significant differences compared with CK1, with increases of 74.09%, 92.14% and 77.74%, respectively (*Fig. 2A,B,D*), while C_i did not show significant differences (*Fig. 2C*). Thus, exogenous spraying of histidine significantly improved maize P_N , g_s and E . Dry weight usually represents the biomass accumulated by the plant, and salt stress significantly reduced the dry weight of maize in this experiment; however, exogenous histidine had no significant effect on maize dry weight under salt stress conditions (*Fig. 2E*). Chlorophyll content is related to a plant's ability to capture light energy, and the relative chlorophyll content of a phanerogamous plant is usually expressed by Chl *a*/Chl *b*. *Fig. 2F* shows a significant decrease in Chl *a*/Chl *b* under salt stress. Histidine caused a significant increase in Chl *a*/Chl *b* by 9.5% under salt stress.

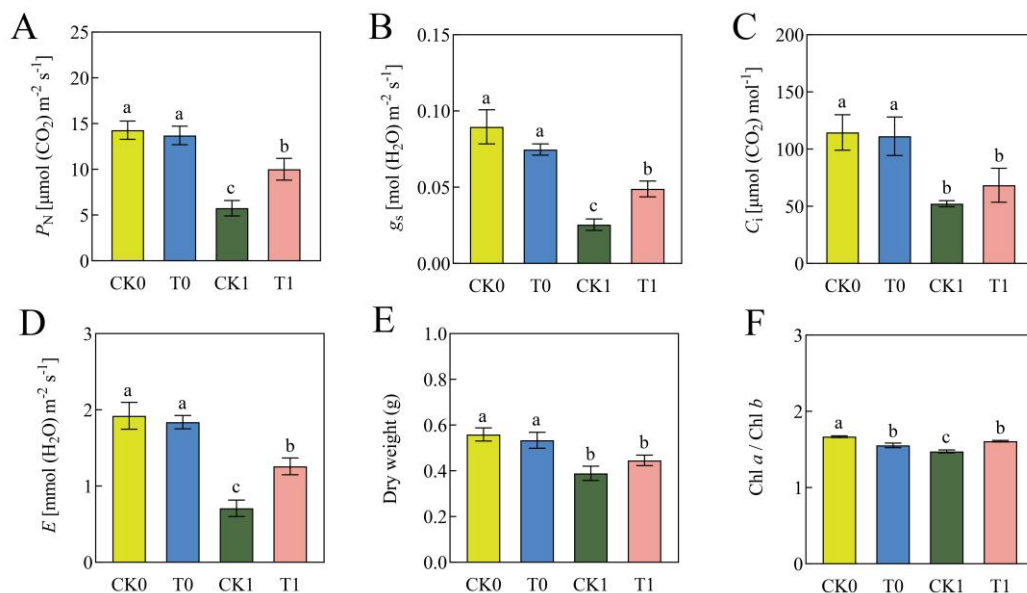


Figure 2. Effect of histidine on photosynthetic performance of maize under salt stress (Duncan test, $p < 0.05$. Bars labeled with different letters for significant differences between treatments were assigned). (A) P_N (net photosynthetic rate); (B) g_s (stomatal conductance); (C) C_i (intercellular CO_2 concentration); (D) E (transpiration rate); (E) Dry weight; (F) Chl a/Chl b (chlorophyll a / chlorophyll b)

Effect of histidine on fluorescence parameters of maize

Chlorophyll fluorescence parameters can reflect the true behavior of photosynthesis in intact plants under stress and can be used as an effective indicator for studying the photochemical efficiency of plants. Fig. 3 shows that under normal conditions, spraying histidine does not affect the fluorescence parameters of maize, while salt stress can significantly change the fluorescence parameters of maize. Under salt stress, F_v/F_m , $\Delta F/F'_m$, and q_p significantly decreased (Fig. 3A,B,C), while NPQ significantly increased (Fig. 3D). It can be seen that after 10 days of salt stress treatment, the photosynthetic mechanism of maize leaves was severely damaged, mainly through increased heat dissipation to consume excess light energy. Under salt stress, exogenous spraying of histidine significantly increased F_v/F_m , $\Delta F/F'_m$ and q_p by 13.8%, 39.1% and 23.2%, respectively (Fig. 3A,B,C), while also significantly reducing the NPQ of maize leaves by 11.4% (Fig. 3D). This indicates that histidine can effectively increase the photochemical activity of the PSII reaction center under salt stress, improving the photochemical efficiency of leaves.

Effect of histidine on the expression of photosynthetic genes and the activity of photosynthetic enzymes in maize

The photosynthetic pathway of plants is affected by environmental conditions, especially the activity of different types of photosynthetic enzymes, which varies with environmental factors. As shown in Fig. 4, under normal conditions, histidine had little effect on the activity of photosynthetic enzymes, and there was no significant difference between the activities of the four enzymes in CK0 and T0. All photosynthetic enzyme activities were affected by salinity, and salt stress significantly decreased the activities

of PEPC, NADP-ME, PPDK, and Rubisco by 64.43%, 41.23%, 50.46%, and 46.77%, respectively. Under salt stress, histidine treatment significantly increased the activity of four photosynthetic enzymes. Compared with CK1, PEPC activity in T1 increased the most significantly, with a significant increase of 73.43% (Fig. 4A). Secondly, the activities of PPDK and NADP-ME in T1 were also significantly different from CK1, with increases of 48.37% and 58.97%, respectively (Fig. 4B,C). Similarly, exogenous histidine treatment under salt stress also significantly increased Rubisco activity, which was 1.8 times higher than CK1 (Fig. 4D). During the conversion process of the plant photosynthetic carbon assimilation pathway, multiple genes are involved in coordinated expression. To further investigate the effect of histidine on maize photosynthesis, we determined the relative expression levels of *ZmPEPC* (LOC542372), *ZmNADP-ME* (LOC542233), *ZmPPDK* (LOC542759), and *ZmRCA* (LOC541712) by RT-qPCR. They can reflect the regulation of histidine on the activity of maize photosynthetic enzymes at the gene level.

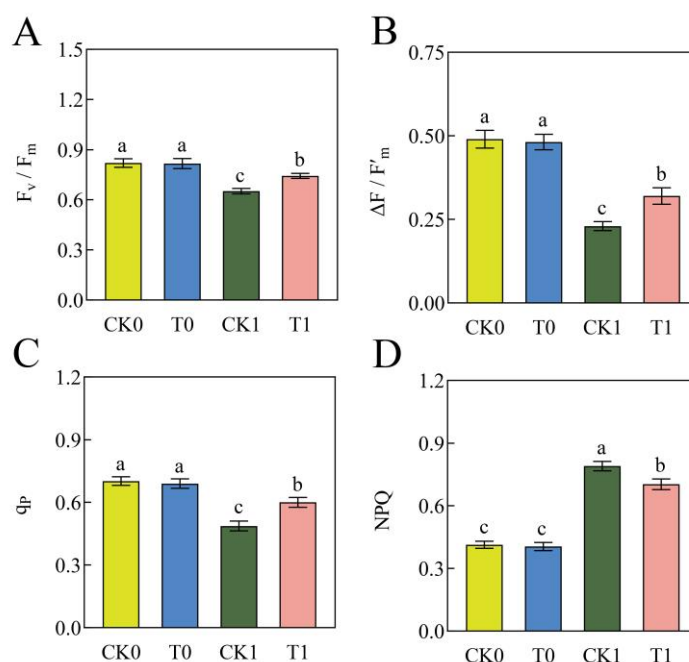


Figure 3. Effect of histidine on chlorophyll fluorescence parameters of maize under salt stress (Duncan test, $p < 0.05$. Bars labeled with different letters for significant differences between treatments were assigned). (A) F_v/F_m (maximum photochemical quantum efficiency of PSII); (B) $\Delta F/F'_m$ (PSII actual photochemical quantum efficiency); (C) q_P (photochemical quenching coefficient); (D) NPQ (non-photochemical quenching coefficient)

In addition, to further explore the relationship between gene expression and enzyme activity, we performed correlation analysis on these four genes and enzymes, establishing a linear regression with the x-axis representing the relative expression of the gene and the y-axis representing the activity of the enzyme. As shown in Fig. 4A, under salt stress, the expression level of *ZmPEPC* significantly increased by 87.37% after treatment with histidine, and there was a significant positive correlation between the relative expression level of *ZmPEPC* and PEPC activity ($r^2 = 0.8867$; $p = 0.005$). Under salt stress, the expression level of *ZmNADP-ME* significantly increased by

46.93% after treatment with histidine (Fig. 4B), and there was a significant positive correlation between the relative expression level of *ZmNADP-ME* and the activity of NADP-ME ($r^2 = 0.8665$; $p = 0.007$). Fig. 4C shows that exogenous histidine treatment significantly up-regulated the expression of *ZmPPDK* under salt stress, with an expression level that was 3.2 times higher than that of CK1. Under salt stress, there was a significant positive correlation between the relative expression level of *ZmPPDK* and PPDK activity after histidine treatment ($r^2 = 0.7557$; $p = 0.0245$). Histidine treatment significantly increased the relative expression level of *ZmRCA* under salt stress, by 243.87% (Fig. 4D), and there was a significant positive correlation between the relative expression level of *ZmRCA* and Rubisco activity ($r^2 = 0.899$; $p = 0.004$).

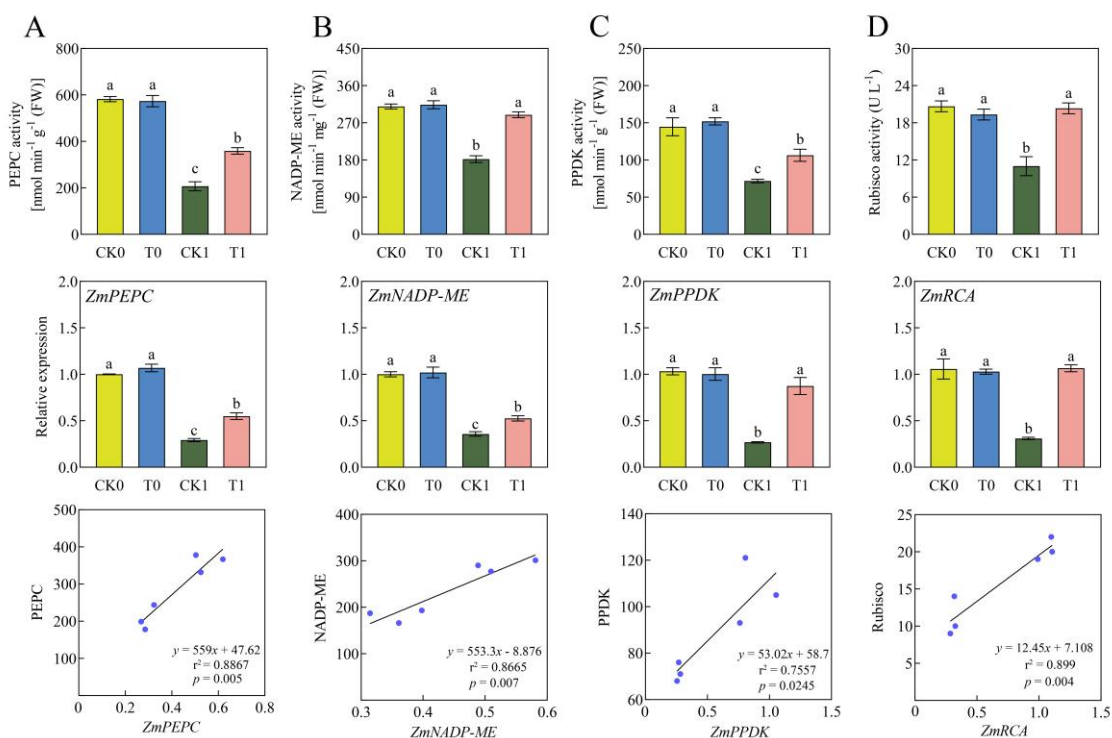


Figure 4. Relative expression of photosynthetic genes and activities of photosynthetic enzymes in maize after histidine treatment (Duncan test, $p < 0.05$. Bars labeled with different letters for significant differences between treatments were assigned) (A) PEPC (phosphoenolpyruvate carboxylase) activity, *ZmPEPC* relative expression and correlation; (B) NADP-ME (NADP-malic enzyme) activity, *ZmNADP-ME* relative expression and correlation; (C) PPDK (phosphoenolpyruvate diphosphokinase) activity, *ZmPPDK* relative expression and correlation; (D) Rubisco (ribulose-1,5-bisphosphate carboxylase), *ZmRCA* (rubisco activase) relative expression and correlation

The effect of histidine spraying on the anatomical structure of maize leaves

In this experiment, cross-sections of maize leaves treated with histidine for 10 days were stained with safranin to observe the leaf cross-sectional structure, and the effect of histidine on the leaf anatomical structure was explored. As shown in Figure 5, scanning software revealed that under normal conditions, exogenous spraying of histidine had a small impact on the anatomical structure of maize leaves, potentially causing a decrease in the length and width of the midvein, the length and width of the vascular bundle, and

leaf thickness, but there were no significant differences compared to CK0 (Fig. 5B). There is no significant difference between CK0 and T0 in terms of the appearance of the bulliform cell, which are both full and intact (Fig. 5A).

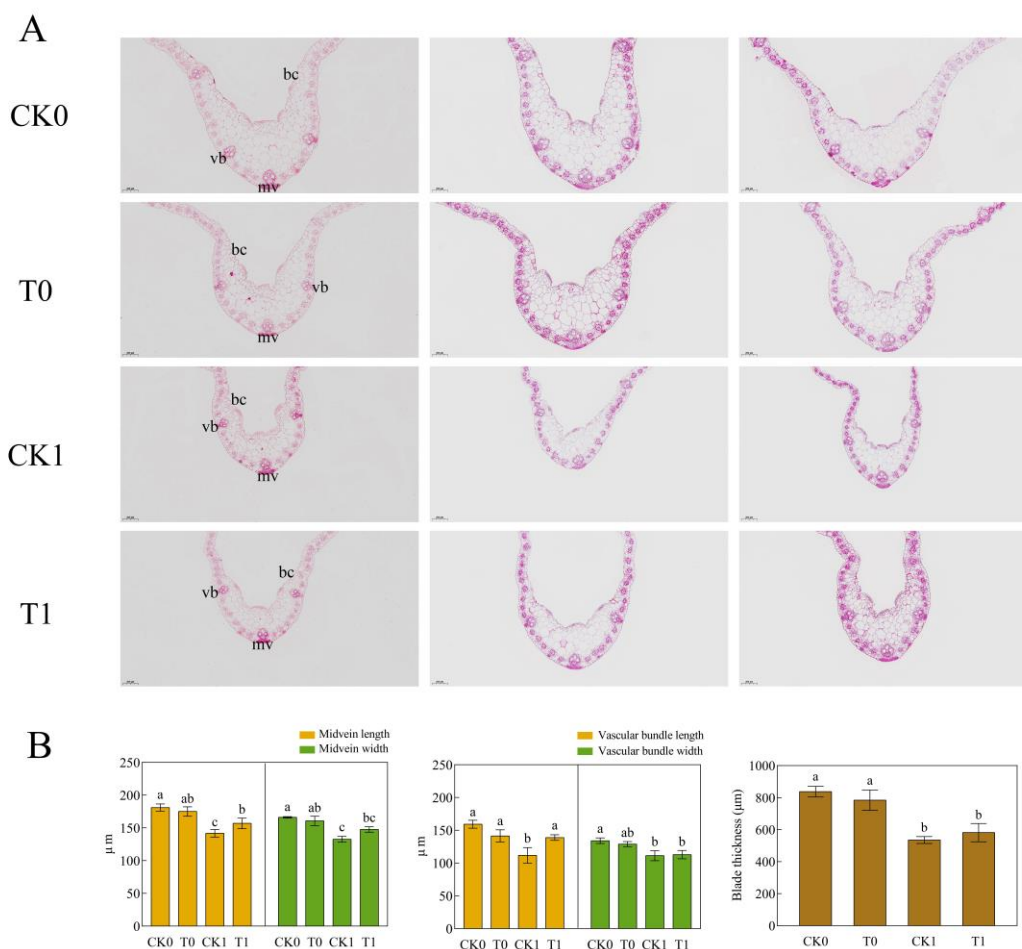


Figure 5. Response of anatomical structure of maize leaves to salt stress and histidine. (A) Cross section of maize leaves for each treatment (bc: bulliform cell, vb: vascular bundle, mv: midvein); (B) Midvein length width, vascular bundle length width, and leaf thickness (Duncan test, $p < 0.05$. Bars labeled with different letters for significant differences between treatments were assigned)

Salt stress significantly affected the morphology of leaf thickness, vascular bundles, and midveins, with significant reductions in leaf thickness, vascular bundle length and width, and midvein length and width compared to CK0 (Fig. 5B). At the same time, leaf vesicular cells collapsed and shrunk (Fig. 5A). Under salt stress, exogenous spraying of histidine significantly improved the morphology of leaves. The length of vascular bundles and midveins increased significantly compared to CK1, by 24.34% and 11.34%, respectively. However, there was no significant difference in vascular bundle width and midvein width between T1 and CK1, and although the leaf thickness increased compared to CK1, there was no significant difference (Fig. 5B). Exogenous histidine can also alleviate the damage caused by salt stress to vacuolate cells and play a certain role in promoting the morphological integrity of vacuolate cells (Fig. 5A).

Discussion

Photosynthesis is crucial for the survival of all biotic communities, playing a key role in plant productivity by generating carbon skeletons. Salt stress can cause irreversible damage to photosynthesis at any stage of development (Zahra et al., 2022). The main factors contributing to the decline in photosynthetic capacity under salt stress include stomatal limitation caused by partial closure of the stomata and non-stomatal limitation caused by a decrease in photosynthetic activity in the mesophyll cells. It is generally believed that when P_N , C_i , and g_s decrease simultaneously, stomatal limitation plays a dominant role; conversely, if the decrease in P_N is accompanied by an increase in C_i , it indicates that the decrease in photosynthesis is mainly due to non-stomatal limitation (Hao et al., 2021). Under salt stress, P_N , g_s , C_i , and E significantly decreased, indicating that the decrease in photosynthesis under salt stress may be caused by stomatal limitations. The results of the experiment showed that spraying 0.5 mM histidine could improve the photosynthetic performance (P_N , g_s , and E) of plants under salt stress. Histidine may improve plant photosynthesis by regulating stomatal conductance. Through the measurement of chlorophyll fluorescence parameters in maize leaves under various treatments, we found that F_v/F_m , $\Delta F/F'_m$, and q_p significantly decreased under salt stress, while NPQ significantly increased. This is because salt stress damages the function of oxygen-evolving complexes, hinders the transfer of electrons from plastid quinone A to plastid quinone B, and leads to a decrease in electron transfer efficiency (Gorbea and Calatayudc, 2013). In addition, salt stress disrupts the lamellar structure of thylakoids and chloroplast grana, reducing chlorophyll content. When spraying histidine under salt stress, F_v/F_m , $\Delta F/F'_m$, q_p , and Chl *a*/Chl *b* significantly increased, while NPQ significantly decreased. Research has shown that exogenous amino acid-derived biological stimulants can improve plant photosynthetic pigments and enhance plants' ability to capture light. Amino acids such as spermine can bind to light complexes to improve the efficiency of electron transfer (Shu et al., 2012b; Hosseini et al., 2022). In addition, gamma-aminobutyric acid can also improve photosynthetic fluorescence parameters in maize under salt stress (Wang et al., 2017). Therefore, histidine can also increase photosynthetic rate by improving photochemical quantum efficiency.

Generally, under high salt stress, the structure of the leaves of plants will change, and the structural changes in the leaves directly affect the physiological and ecological functions of the plants (Shen et al., 2022). Therefore, understanding the response of leaf structure to the environment is an important foundation for exploring plant adaptation mechanisms. Xylem transports water and inorganic nutrients for photosynthesis, while phloem transports photosynthetic products and signaling molecules from the mesophyll to other parts of the plant. The vascular bundle is composed of xylem and phloem (Sun et al., 2022). As a monocot plant, the degree of development of the midrib in maize can determine the degree of water and nutrient transport. The results of the experiment showed that the length and width of vascular bundles and midveins significantly decreased under salt stress. The reduction in vascular bundles greatly weakened the conductivity of xylem and phloem, reducing the transport of nutrients and water in the soil (Ajuziogu et al., 2019). After spraying histidine, the length of vascular bundles and midveins in leaves significantly increased, which enhanced water transport and nutrient accumulation. Research has found that drought and salt stress can cause plant leaves to curl, and vesicular cells form longitudinal stripes on the adaxial leaf surface, causing the leaves to curl or fold up through water absorption and loss, which is related to plant drought and salt resistance (Matschi et al., 2020). Under salt stress, the leaf vesicular

cells treated with histidine gradually become full of shrinkage and dehydration, which can alleviate leaf curling and expand the area of photosynthesis.

Rubisco is the most abundant soluble protein in leaves, and its activity directly affects photosynthetic rate (Spreitzer and Salvucci, 2002). However, the catalytic efficiency of Rubisco carboxylase in plants is very low, and it can only maintain high catalytic activity when Rubisco activase (RCA) is present (Portis, 2014). The decrease in Rubisco activity is often considered as one of the non-stomatal factors that lead to a decrease in photosynthesis (Delfine et al., 1999). Under salt stress, the expression of *ZmRCA* and Rubisco activity were significantly increased by exogenous spraying of histidine, directly improving the photosynthetic rate of plants. PEPC, NADP-ME, and PPDK are all involved in CO₂ fixation in C₄ photosynthesis and are important enzyme proteins in higher plants (Glackin and Grula, 1990; Abdel-Latif, 2008). PPDK is related to the regeneration rate of PEP in the C₄ pathway. After treatment with histidine under salt stress, PPDK activity and *ZmPPDK* expression were significantly increased. PEPC regulates respiratory carbon flux and thus affects nitrogen assimilation, thus playing a crucial role in carbon and nitrogen metabolism (Shi et al., 2015). Studies have found that the PEPC gene can be genetically modified to improve photosynthesis and thereby respond to abiotic stress performance and adaptability (Jeanneau et al., 2002). The PEPC activity and *ZmPEPC* expression level were significantly increased after histidine treatment under salt stress. NADP-ME can improve the ability of plants to resist salt stress by enhancing their carbon fixation capacity. Research has shown that NADP-ME is involved in the response of cucumber plants to salt and osmotic stress (Hýsková et al., 2017). After treatment with histidine under salt stress, NADP-ME activity and *ZmNADP-ME* expression were significantly increased. Therefore, histidine may be similar to other biological stimulants, enhancing the expression of photosynthetic genes, thereby increasing the activity of photosynthetic enzymes and increasing the assimilation efficiency of CO₂ in both C₄ and C₃ pathways.

Conclusion

Spraying histidine under salt stress changes the fluorescence parameters, improves the efficiency of electron transfer, enhances the expression of photosynthetic genes, regulates the activity of photosynthetic enzymes, enhances the carbon fixation process and the synthesis of organic matter in plants, and significantly improves the photosynthetic performance of maize leaves under salt stress. Therefore, histidine has certain application potential and can be used as a biostimulant for salt tolerance in maize.

Acknowledgements. This research was funded by the Ningxia Key Research and Development Plan (2023BCF01014), the National Natural Science Foundation of China (32060424), Science and Technology Leading Talents of Ningxia Hui Autonomous Region (2022GKLRLX06).

Conflict of interests. The authors declare that there is no conflict of interests.

REFERENCES

- [1] Abdel-Latif, A. (2008): Phosphoenolpyruvate carboxylase activity of wheat and maize seedlings subjected to salt stress. – Australian Journal of Basic and Applied Sciences 2(1): 37-41.
- [2] Ajuziogu, G. C., Abu, N. E., Aino, D. O., Ideyi, S., Udoh, O. E., Ojua, E. O. (2019): Effect of crude oil concentrations on the vascular bundle size of two maize varieties. – International Journal of Plant and Soil Science 30(5): 1-6.
- [3] Çavuşoğlu, K., Kilic, S., Kabar, K. (2018): Effects of some plant growth regulators on stem anatomy of radish seedlings grown under saline (NaCl) conditions. – Plant Soil and Environment 54: 428-433.
- [4] Delfine, S., Alvino, A., Villani, M. C., Loreto, F. (1999): Restrictions to carbon dioxide conductance and photosynthesis in spinach leaves recovering from salt stress. – Plant Physiology 119(3): 1101-1106.
- [5] Du, Y., Zhao, M., Wang, C., Gao, Y., Wang, Y., Liu, Y., Chen, M., Chen, J., Zhou, Y., Xu, Z., Ma, Y. (2018): Identification and characterization of GmMYB118 responses to drought and salt stress. – BMC Plant Biology 18.
- [6] Fernandez-Garcia, N., Olmos, E., Bardisi, E., García-De la Garma, J., López-Berenguer, C., Rubio-Asensio, J. S. (2014): Intrinsic water use efficiency controls the adaptation to high salinity in a semi-arid adapted plant, henna (*Lawsonia inermis* L.). – Journal of Plant Physiology 171(5): 64-75.
- [7] Glackin, C. A., Gula, J. W. (1990): Organ-specific transcripts of different size and abundance derive from the same pyruvate, orthophosphate dikinase gene in maize. – Proceedings of the National Academy of Sciences of the United States of America 87: 3004-3008.
- [8] Gorbea, E., Calatayud, A. (2013): Applications of chlorophyll fluorescence imaging technique in horticultural research: a review. – Scientia Horticulturae 99(2): 24-35.
- [9] Hao, S., Wang, Y., Yan, Y., Liu, Y., Wang, J., Chen, S. (2021): A review on plant responses to salt stress and their mechanisms of salt resistance. – Horticulturae 7: 132.
- [10] Hassani, A., Azapagic, A., Shokri, N. (2020): Predicting long-term dynamics of soil salinity and sodicity on a global scale. – Proceedings of the National Academy of Sciences of the United States of America 117: 33017-33027.
- [11] Hosseini, S., Shabani, L., Sabzalian, M. R., Gharibi, S. (2022): Foliar spray of commercial seaweed and amino acid-derived biostimulants promoted phytoremediation potential and salinity stress tolerance in halophytic grass, *Puccinellia distans*. – International Journal of Phytoremediation 25: 415-429.
- [12] Hýšková, V., Plisková, V., Červený, V., Ryšlavá, H. (2017): NADP-dependent enzymes are involved in response to salt and hypoosmotic stress in cucumber plants. – General Physiology and Biophysics 36(3): 247-258.
- [13] Ilangumaran, G., Smith, D. L. (2017): Plant growth promoting rhizobacteria in amelioration of salinity stress: a systems biology perspective. – Frontiers in Plant Science 8.
- [14] Ioannidis, N., Sfichi, L., Kotzabasis, K. (2006): Putrescine stimulates chemiosmotic ATP synthesis. – Biochimica et Biophysica Acta 1757(7): 821-828.
- [15] Irtelli, B., Petrucci, W. A., Navari-Izzo, F. (2008): Nicotianamine and histidine/proline are, respectively, the most important copper chelators in xylem sap of *Brassica carinata* under conditions of copper deficiency and excess. – Journal of Experimental Botany 60(1): 269-277.
- [16] Jeanneau, M., Vidal, J., Gousset-dupont, A., Lebouteiller, B., Hodges, M., Gerentes, D., Perez, P. (2002): Manipulating PEPC levels in plants. – Journal of Experimental Botany 53(376): 1837-1845.

- [17] Ji, X., Cheng, J., Gong, D., Zhao, X., Qi, Y., Su, Y., Ma, W. (2018): The effect of NaCl stress on photosynthetic efficiency and lipid production in freshwater microalga-*scenedesmus obliquus* XJ002. – *The Science of the Total Environment* 633: 593-599.
- [18] Ji, H., Yang, G., Zhang, X., Zhong, Q., Qi, Y., Wu, K., Shen, T. (2022): Regulation of salt tolerance in the roots of *Zea mays* by L-histidine through transcriptome analysis. – *Frontiers in Plant Science* 13.
- [19] Krämer, U., Cotter-Howells, J. D., Charnock, J. M., Baker, A. J., Smith, J. A. (1996): Free histidine as a metal chelator in plants that accumulate nickel. – *Nature* 379: 635-638.
- [20] Lichtenthaler, H. K., Wellburn, A. R. (1983): Determinations of total carotenoids and chlorophylls a and b of leaf extracts in different solvents. – *Biochemical Society Transactions* 11: 591-592.
- [21] Matschi, S., Vasquez, M. F., Bourgault, R., Steinbach, P. A., Chamness, J. C., Kaczmar, N., Gore, M. A., Molina, I., Smith, L. G. (2020): Structure-function analysis of the maize bulliform cell cuticle and its potential role in dehydration and leaf rolling. – *Plant Direct* 4(10): 1-21.
- [22] Noutoshi, Y., Ito, T., Shinozaki, K. (2005): Albino and pale green 10 encodes BBMII isomerase involved in histidine biosynthesis in *Arabidopsis thaliana*. – *Plant and Cell Physiology* 46(7): 1165-1172.
- [23] Othman, Y. A., Al-Karaki, G. N., Al-Horani, A. S. (2006): Variation in germination and ion uptake in barley genotypes under salinity conditions. – *World Journal of Agricultural Sciences* 2(1): 11-15.
- [24] Portis, A. R. (2004): Rubisco activase-rubisco's catalytic chaperone. – *Photosynthesis Research* 75: 11-27.
- [25] Shen, Z., Cheng, X., Li, X., Deng, X., Dong, X., Wang, S. J., Pu, X. (2022): Effects of silicon application on leaf structure and physiological characteristics of *Glycyrrhiza uralensis* Fisch. and *Glycyrrhiza inflata* Bat. under salt treatment. – *BMC Plant Biology* 22: 390.
- [26] Shi, J., Yi, K., Liu, Y., Xie, L., Zhou, Z., Chen, Y., Hu, Z., Zheng, T., Liu, R., Chen, Y., Chen, J. (2015): Phosphoenolpyruvate carboxylase in *Arabidopsis* leaves plays a crucial role in carbon and nitrogen metabolism. – *Plant Physiology* 167(3): 671-681.
- [27] Shu, S., Guo, S., Sun, J., Yuan, L. (2012a): Effects of salt stress on the structure and function of the photosynthetic apparatus in *Cucumis sativus* and its protection by exogenous putrescine. – *Physiologia Plantarum* 146(3): 285-296.
- [28] Shu, S., Yuan, L., Guo, S., Sun, J., Liu, C. (2012b): Effects of exogenous spermidine on photosynthesis, xanthophyll cycle and endogenous polyamines in cucumber seedlings exposed to salinity. – *African Journal of Biotechnology* 11(22): 6064-6074.
- [29] Shu, S., Chen, L., Lu, W., Sun, J., Guo, S., Yuan, Y., Li, J. (2014): Effects of exogenous spermidine on photosynthetic capacity and expression of Calvin cycle genes in salt-stressed cucumber seedlings. – *Journal of Plant Research* 127: 763-773.
- [30] Spreitzer, R. J., Salvucci, M. E. (2002): Rubisco: structure, regulatory interactions, and possibilities for a better enzyme. – *Annual Review of Plant Biology* 53: 449-475.
- [31] Stepansky, A., Leustek, T. (2006): Histidine biosynthesis in plants. – *Amino Acids* 30(2): 127-142.
- [32] Sudhir, P., Murthy, S. D. (2004): Effects of salt stress on basic processes of photosynthesis. – *Photosynthetica* 42: 481-486.
- [33] Sun, G., Zhang, X., Duan, H., Gao, J., Li, N., Su, P., Xie, H., Li, W., Fu, Z., Huang, Y., Tang, J. (2022): Dissection of the genetic architecture of peduncle vascular bundle-related traits in maize by a genome-wide association study. – *Plant Biotechnology Journal* 20: 1042-1053.
- [34] Tang, X., Mu, X., Shao, H., Wang, H., Brestič, M. (2015): Global plant-responding mechanisms to salt stress: physiological and molecular levels and implications in biotechnology. – *Critical Reviews in Biotechnology* 35(4): 425-437.

- [35] Turan, S., Tripathy, B. C. (2014): Salt-stress induced modulation of chlorophyll biosynthesis during de-etiolation of rice seedlings. – *Physiologia Plantarum* 153(3): 477-491.
- [36] Wang, Y., Gu, W., Meng, Y., Xie, T., Li, L., Li, J., Wei, S. (2017): γ -aminobutyric acid imparts partial protection from salt stress injury to maize seedlings by improving photosynthesis and upregulating osmoprotectants and antioxidants. – *Scientific Reports* 7: 43609.
- [37] Zahra, N., Al Hinai, M. S., Hafeez, M. B., Rehman, A., Wahid, A., Siddique, K. H., Farooq, M. (2022): Regulation of photosynthesis under salt stress and associated tolerance mechanisms. – *Plant Physiology and Biochemistry* 178: 55-69.
- [38] Zhang, H., Liu, S., Ma, J., Wang, X., Haq, S. U., Meng, Y., Zhang, Y., Chen, R. (2019): CaDHN4, a salt and cold stress-responsive dehydrin gene from pepper decreases abscisic acid sensitivity in *Arabidopsis*. – *International Journal of Molecular Sciences* 21: 26.

APPENDIX

Table S1. *Primer sequences for photosynthetic enzyme related genes*

Gene name	Forward primer	Reverse primer
ZmGAPDH	AGC ACA GCG ACA TCA CAC TC	AAC AAC CTT CTT GGC ACC AC
ZmPEPC	AGC TCC ACA GTT CGT CTG GT	GCT CAA GTG GCT CAA GGA AC
ZmPPDK	TAC CTC TCA GCC AAG GGA GA	AGA AGT GTT CCC CAT GTT GC
ZmNADP-ME	GTG GTC CTT GCA GGT TTG TT	TGA AGG GAG CCT TTA CGA GA
ZmRCA	AGG AAG CTC GTC AAC TCC AA	AGA GCA GCC TCG TTG AGG TA